Translational Oncology
www.transonc.com

Volume 7 Number 2 April 2014 pp. 256–266.e5 256

PI3K Inhibition Augments the Therapeutic Efficacy of a 3a-aza-Cyclopenta[α]indene Derivative in Lung Cancer Cells[1,2]

Kumar Sanjiv[*,†], Chi-Wei Chen[‡,§], Rajesh Kakadiya[§], Satishkumar Tala[§], Sharda Suman[§], Ming-Hsi Wu[§], Yen-Hui Chen[§], Tsann-Long Su[*,§,¶] and Te-Chang Lee[*,‡,§]

*Molecular Medicine Program, Taiwan International Graduate Program, Academia Sinica, Taipei, Taiwan; †Institute of Biochemistry and Molecular Biology, National Yang-Ming University, Taipei, Taiwan; ‡Institute of Biopharmaceutical Sciences, National Yang-Ming University, Taipei, Taiwan; §Institute of Biomedical Sciences, Academia Sinica, Taipei, Taiwan; ¶Graduate Institute of Pharmaceutical Chemistry, China Medical University, Taichung, Taiwan

Abstract

The synergistic targeting of DNA damage and DNA repair is a promising strategy for the development of new chemotherapeutic agents for human lung cancer. The DNA interstrand cross-linking agent BO-1509, a derivative of 3a-aza-cyclopenta[α]indene, was synthesized and combined with the phosphoinositide 3-kinase (PI3K) inhibitor LY294002 to treat human lung cancer cells. Our results showed that the BO-1509 and LY294002 combination synergistically killed lung cancer cells in culture and also suppressed the growth of lung cancer xenografts in mice, including those derived from gefitinib-resistant cells. We also found that LY294002 suppressed the induction of several DNA repair proteins by BO-1509 and inhibited the nuclear translocation of Rad51. On the basis of the results of the γH2AX foci formation assays, LY294002 apparently inhibited the repair of DNA damage that was induced by BO-1509. According to the complete blood profile, biochemical enzyme analysis, and histopathologic analysis of major organs, no apparent toxicity was observed in mice treated with BO-1509 alone or in combination with LY294002. Our results suggest that the combination of a DNA cross-linking agent with a PI3K inhibitor is a feasible strategy for the treatment of patients with lung cancer.

Translational Oncology (2014) 7, 256–266.e5

Introduction

DNA-damaging agents have been used to treat various cancers, including lung cancer, since World War II [1]. Numerous bifunctional DNA-damaging agents, including platinum complexes (cisplatin and oxaliplatin) and nitrogen mustards (mustine, chlorambucil, and melphalan), are still widely used in the treatment of a variety of cancers [2,3]. These bifunctional alkylating agents induce a variety of DNA lesions, including DNA interstrand cross-links (ICLs) that subsequently generate double-strand breaks (DSBs), stop DNA synthesis, and trigger cell death [4]. Several novel ICL-inducing agents are under development for use as cancer therapeutics [5]. However, various signaling pathways and repair mechanisms that comprise the DNA damage response (DDR) are activated to counteract the effects of DNA damage [6]. Many studies have shown that enhanced DNA repair activity contributes to chemotherapeutic resistance [1,4,7]. Thus, the targeting of DNA repair is a promising approach for the development of new chemotherapeutic agents that are capable of overcoming drug resistance [8].

Address all correspondence to: Te-Chang Lee, PhD or Tsann-Long Su, PhD, Institute of Biomedical Sciences, Academia Sinica, Taipei 11529, Taiwan. E-mail: tlsu@ibms.sinica.edu.tw

[1] This work was supported by a Thematic Project Program grant from Academia Sinica, Taipei, Taiwan (AS-100-TP-B13 to T.C.L. and T.L.S.) and a National Research Program for Biopharmaceuticals grant from the National Science Council, Taipei, Taiwan (NSC 100-2325-B-001-003). Statement of conflicts of interest: No potential conflicts of interest are disclosed.

[2] This article refers to supplementary materials, which are designated by Table W1 and Figures W1 to W5 and are available online at www.transonc.com.

Received 2 September 2013; Revised 3 January 2014; Accepted 30 January 2014

http://dx.doi.org/10.1016/j.tranon.2014.02.012

The PI3K/AKT pathway has been well characterized as a signaling pathway that promotes cell survival [9]. Numerous studies have also shown that the PI3K/AKT signaling pathway regulates the Mre11-Rad50-Nbs1 (MRN) complex and the Rad51 protein, which are essential components of DSB repair, through homologous recombination (HR) and nonhomologous end joining (NHEJ), respectively [10-13]. In response to DNA damage, the protein ataxia-telangiectasia mutated (ATM), which is a member of the PI3K family of serine-threonine kinases, phosphorylates the Nbs1 component of the MRN complex [14,15]. Recently, great emphasis has been placed on developing inhibitors of this pathway with the goal of improving therapeutic efficacy [16]. Many specific inhibitors of PI3K isoforms have been used in clinical trials [11,16-19]. LY294002, the first synthetic inhibitor that targets all of the isoforms of P110, displays little or no selectivity for individual isoforms of PI3K and ATM [16,20]. LY294002 has been studied in preclinical ovarian, colon, pancreatic, and nasopharyngeal cancer models [17,21-24]. LY294002 has also been used in combination with chemotherapeutic agents and ionizing radiation [18,25-27]. Although the use of LY294002 is limited because of its toxicity and low solubility, it has been used extensively in various *in vitro* and *in vivo* systems to evaluate the biologic significance of PI3K [16].

We have previously designed and synthesized several series of bifunctional alkylating agents that were found to have potent activity against a variety of cancer xenograft models [28-30]. Among these agents, the compound BO-1012 (Figure W1*A*), which is a bis (methylcarbamate) derivative of 3a-aza-cyclopenta[α]indene, was shown to have potent therapeutic efficacy against inherited resistance H460 cells and bladder cancer cells with acquired cisplatin resistance (NTUB1/P) in nude mice when used in combination with arsenic trioxide [31]. Another derivative, BO-1090, was found to be effective against a variety of oral cancer cells both *in vitro* and *in vivo* [30]. Compound BO-1012 displays potent therapeutic efficacy and was selected as a lead compound for further development as an antitumor agent. However, this agent was not suitable for large-scale preparation because of the explosive and severely hazardous properties of methyl isocyanate, which was used to introduce the bis(methylcarbamate) functional group into the final product. For lead optimization, we synthesized compound 3-(4-methoxyphenyl)-9*H*-pyrrolo[1,2-*a*]indole-1,2-diyl)bis(methylene) bis(ethylcarbamate) (BO-1509) (Figure W1), which bears a bis(ethylcarbamate) group and can be prepared in large amounts. Notably, we found that BO-1509 possessed the ability to kill various cancer cell lines.

ICLs formed by bifunctional alkylating agents are usually repaired by a complex pathway [32]. The combination of a PI3K inhibitor with an anticancer agent is therefore believed to increase the efficacy of the drug or to decrease drug resistance [33,34]. In this study, we investigated the anticancer activity of BO-1509 in combination with LY294002 against non–small cell lung cancer (NSCLC), which accounts for approximately 80% of lung cancer cases [35]. More than half of patients with NSCLC have epidermal growth factor receptor (EGFR) mutations and are promisingly treated with tyrosine kinase inhibitors (TKIs), such as erlotinib or gefitinib [36-39]. Unfortunately, the emergence of resistance to targeted therapeutics occurs nearly in all patients in a short period [40]. Therefore, in this study, we demonstrated that the combination of BO-1509 with LY294002 significantly suppressed the growth of several lung cancer cell lines, including EGFR-mutant NSCLC lines, PC9 and PC9/gef B4 cells, both *in vitro* and *in vivo*.

Materials and Methods

Cell Lines and Cell Culture

H460 and A549 cells were obtained from the American Type Culture Collection (Manassas, VA). Gefitinib-sensitive (PC9) and gefitinib-resistant (PC9/gef B4) cells were kindly provided by Dr Chih-Hsin Yang (Department of Oncology, National Taiwan University Hospital, Taipei, Taiwan) [41]. CL1-5, CL83, and CL25 cells were provided by Dr Pan-Chyr Yang (Department of Internal Medicine, National Taiwan University Hospital, Taipei, Taiwan) [42]. A549 cells were maintained in Dulbecco's modified Eagle's medium. All other cells were cultured in RPMI 1640 supplemented with 10% FBS and incubated at 37°C in 5% CO_2. The characteristics of these cell lines are listed in Table W1.

Chemicals

BO-1509 (3-(4-methoxyphenyl)-9*H*-pyrrolo[1,2-*a*]indole-1,2-diyl)bis(methylene) bis(ethylcarbamate) was synthesized as previously described [28]. The PI3K inhibitor LY294002 was purchased from Cayman Chemical Company (Ann Arbor, MI).

Drug Treatment and Cytotoxicity Assays

For the cytotoxicity assays, 3000 cells were seeded into each well of a 96-well plate, incubated overnight at 37°C, and then treated for 72 hours with various concentrations of BO-1509, LY294002, or a combination of both compounds. At the end of the treatment, 20 μl of Alamar Blue solution (AbD Serotec, Kidlington, United Kingdom) was added to each well and then incubated for 6 hours. Cell viability was assessed by measuring the absorbance at 570 and 600 nm according to the manufacturer's instructions. The concentration of drug that resulted in a 50% inhibition of cell growth (IC_{50}) was determined for each drug, and the combination index (CI) was determined using the CompuSyn software (version 1.0.1; CompuSyn, Inc, Paramus, NJ) and the median effect principle and plot [43]. The IC_{50} values were presented as means ± SD of three independent experiments.

Western Blot Analysis

Western blot analysis was performed as previously described [29] and was adopted to determine the intracellular protein levels in response to drug treatment. Briefly, cells were harvested after drug treatment and lysed in electrophoresis sample buffer. Proteins were then electrophoretically separated on a sodium dodecyl sulfate–polyacrylamide gel and transferred onto polyvinylidene difluoride membranes (Amersham Biosciences, GE Healthcare Bio-Sciences Corp, Piscataway, NJ). Protein-conjugated membranes were incubated with primary antibodies overnight at 4°C and then incubated with HRP-conjugated anti-rabbit or anti-mouse secondary antibody for 1 hour at room temperature. Western blot signals were visualized by chemiluminescence using SuperSignal West Pico chemiluminescence reagent (Pierce, Rockford, IL). Antibodies against AKT, phospho-AKT, Mre11, and FANCD2 were obtained from Santa Cruz Biotechnology (Dallas, TX), whereas antibodies against Nbs1, phospho-Nbs1 (pNbs1), Rad50, Rad51, and β-actin were from Genetex (San Antonio, TX). Antibodies against caspase-3, caspase-7, and poly(ADP-ribose) polymerase (PARP) and secondary antibodies

against rabbit and mouse Ig were purchased from Cell Signaling Technology (Danver, MA). The anti-γH2AX antibody was obtained from Millipore (Billerica, MA).

Apoptosis Assays

The induction of apoptosis by the treatment of cells with BO-1509, LY294002, or a combination of both agents was detected by flow cytometry using 4′,6-diamidino-2-phenylindole (DAPI) staining (1 μg/ml; Merck Millipore, Darmstadt, Germany) and the Annexin V–FITC Apoptosis Detection Kit (Calbiochem, La Jolla, CA) according to the manufacturer's instructions.

Immunofluorescence Staining

Immunofluorescence staining was used to detect the formation of γH2AX foci and the nuclear translocation of Rad51 as previously described [30,31]. The nucleus was counterstained with DAPI. After staining, cells were examined using a confocal microscope (LSM 510; Carl Zeiss Microscopy Ltd, Cambridge, United Kingdom). Cells with at least five γH2AX foci in the nucleus were considered to be positive for the formation of γH2AX foci [44].

Mouse Xenograft Models

The use of mouse xenograft models for the analysis of tumor suppression followed the guidelines approved by the Institutional Animal Care and Utilization Committee of the Academia Sinica (Taipei, Taiwan). Six-week-old male BALB/c nude mice were obtained from the National Laboratory Animal Center (Taipei, Taiwan) and housed in a specific pathogen-free environment under controlled conditions of light and humidity as previously described [30,31]. To generate the xenografts, tumor cells (approximately 3×10^6 to 5×10^6 cells) suspended in 100 μl of phosphate-buffered saline were inoculated subcutaneously into the flank region of mice. When the tumor size reached approximately 100 mm^3, mice were randomly divided into four groups and treated with vehicle, BO-1509 (5 mg/kg body weight), LY294002 (40 mg/kg body weight), or a combination of both BO-1509 and LY294002. BO-1509 and LY294002 were prepared in 0.9% saline containing 8% DMSO, 6% Tween-80, and 16% cremophor [25]. BO-1509 was injected intravenously (i.v.) five times on alternate days (days 0, 2, 4, 6, and 8), whereas LY294002 was given by intraperitoneal (i.p.) injection everyday for 9 days. Tumor volume (mm^3) was measured using

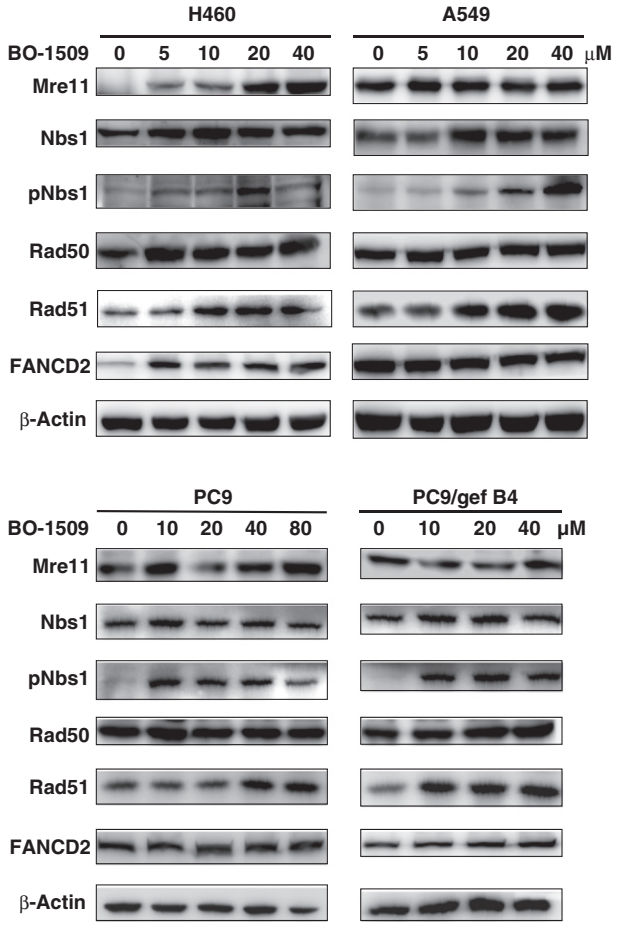

Figure 1. Activation of repair proteins in BO-1509–treated lung cancer cells. H460, A549, PC9, and PC9/gef B4 cells were treated with various concentrations (10-80 μM) of BO-1509 for 24 hours. The levels of the DNA repair proteins in cell lysates were analyzed by Western blot analysis. β-Actin was included as a loading control.

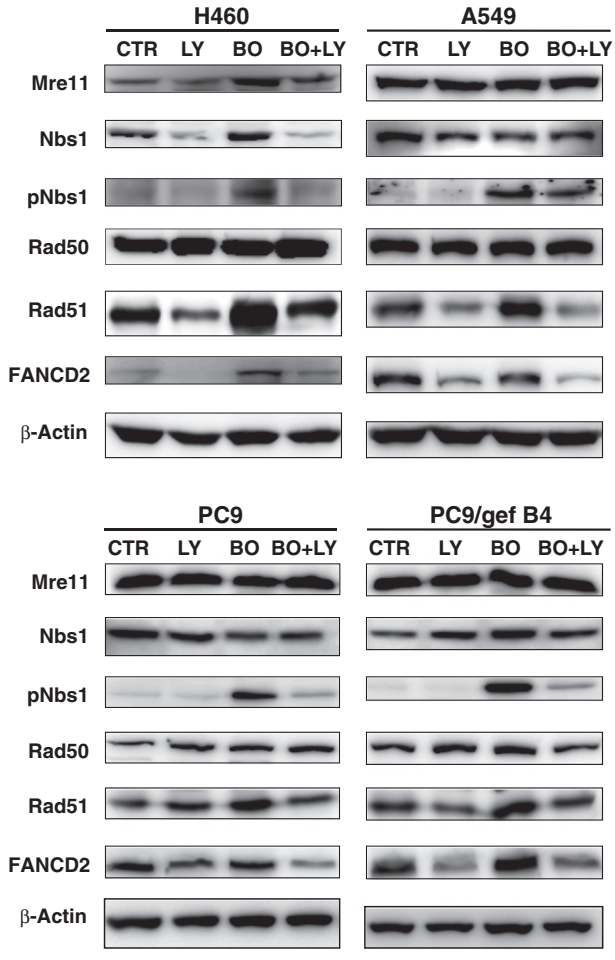

Figure 2. Suppression of BO-1509–mediated activation of DNA repair proteins in various lung cancer cells. H460, A549, PC9, and PC9/gef B4 cells were treated with 20 μM BO-1509 or 40 μM LY294002 alone or in combination for 24 hours. The levels of the DNA repair proteins in the cell lysates were analyzed by Western blot analysis. β-Actin was included as a loading control.

calipers and calculated according to the following formula: tumor volume = (length × width^2)/2.

Whole Blood, Biochemical Parameters, and Histopathology

The effects of the drug treatment on the biochemical and cellular characteristics of the blood and on the histopathology of various organs were analyzed as previously described [30]. Briefly, 1 day after the last i.v. injection, hematological and biochemical parameters and the histopathology of the liver, kidney, lung, and spleen in mice treated with BO-1509 and LY294002 were examined at the Taiwan Mouse Clinic and the Pathology Core of the Institute of Biomedical Sciences at the Academia Sinica, respectively.

Results

DNA Damage Response in Lung Cancer Cells Treated with BO-1509

Because BO-1509 is a newly synthesized DNA cross-linking agent (Figure W1), we measured the cytotoxicity of BO-1509 in several lung cancer cell lines using the Alamar Blue assay. Treatment of cell lines with BO-1509 for 72 hours allowed the determination of IC_{50} values of BO-1509 in each of the following cell lines: H460 (17.5 ± 3.7 μM), A549 (15.5 ± 3.5 μM), PC9 (82.7 ± 2.6 μM), PC9/gef B4 (57.7 ± 3.4 μM), CL1-5 (26.5 ± 5.4 μM), CL25 (17.1 ± 3.2 μM), and CL83 (19.5 ± 2.5 μM). To evaluate the effects of BO-1509 on the DDR in these lung cancer cells, we treated the cells with various concentrations of BO-1509 for 24 hours. Because most of the cells remained intact, we then examined the levels of several proteins involved in HR and NHEJ repair (Figure 1). Mre11 was induced in a concentration-dependent manner in H460 cells but was not significantly induced in other cell lines. Although the protein levels of Nbs1 were only slightly increased upon treatment with BO-1509, protein levels of pNbs1, the active form of Nbs1, were significantly elevated in all four cell lines examined. BO-1509 treatment did not result in a significant change in Rad50 protein levels in any of the cell lines. In contrast, the protein levels of Rad51 were increased in a concentration-dependent manner in four of the cell lines after treatment with BO-1509. An

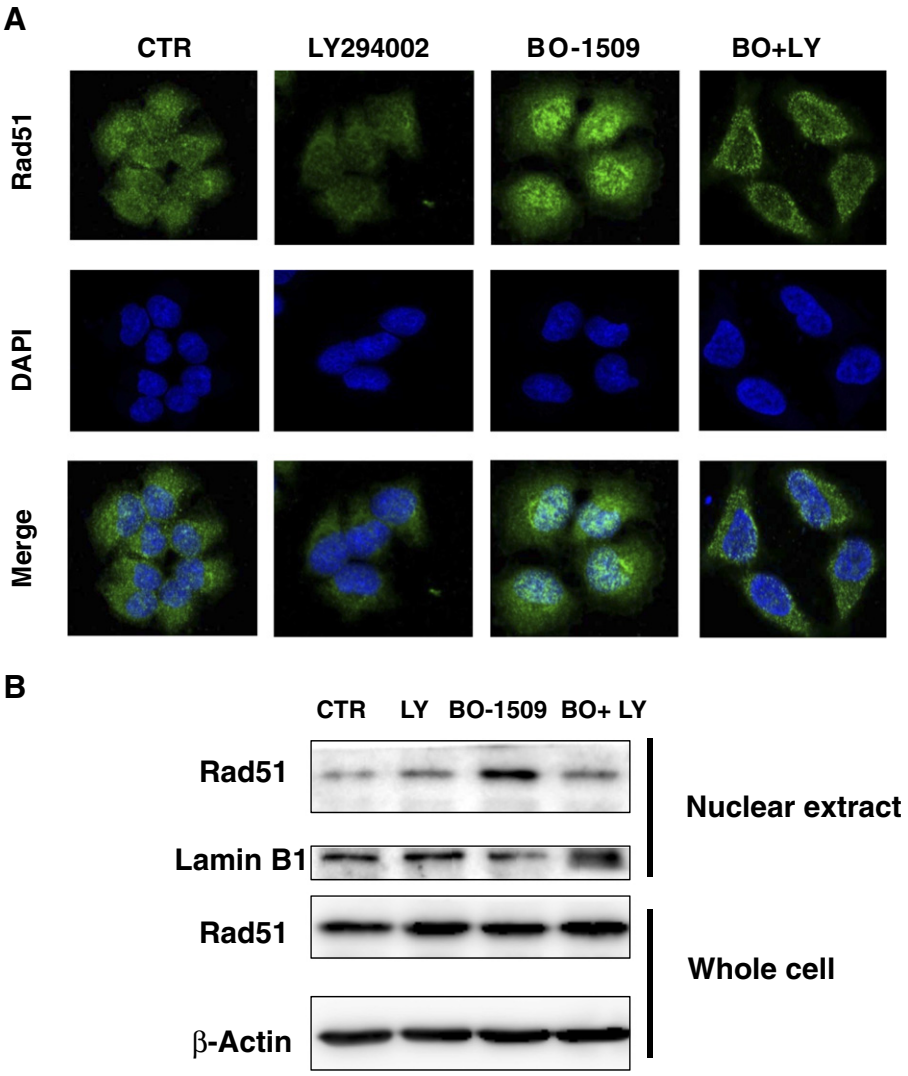

Figure 3. Inhibition of BO-1509–mediated Rad51 foci formation in nuclei of H460 cells. H460 cells grown on chamber slides were treated with 20 μM BO-1509 for 2 hours, followed by treatment with or without 40 μM LY294002 for 24 hours. At the end of the incubation, the cells were fixed and stained with a primary antibody against Rad51, followed by an Alexa Fluor 488–conjugated secondary antibody (green). Nuclei were counterstained with DAPI (blue).

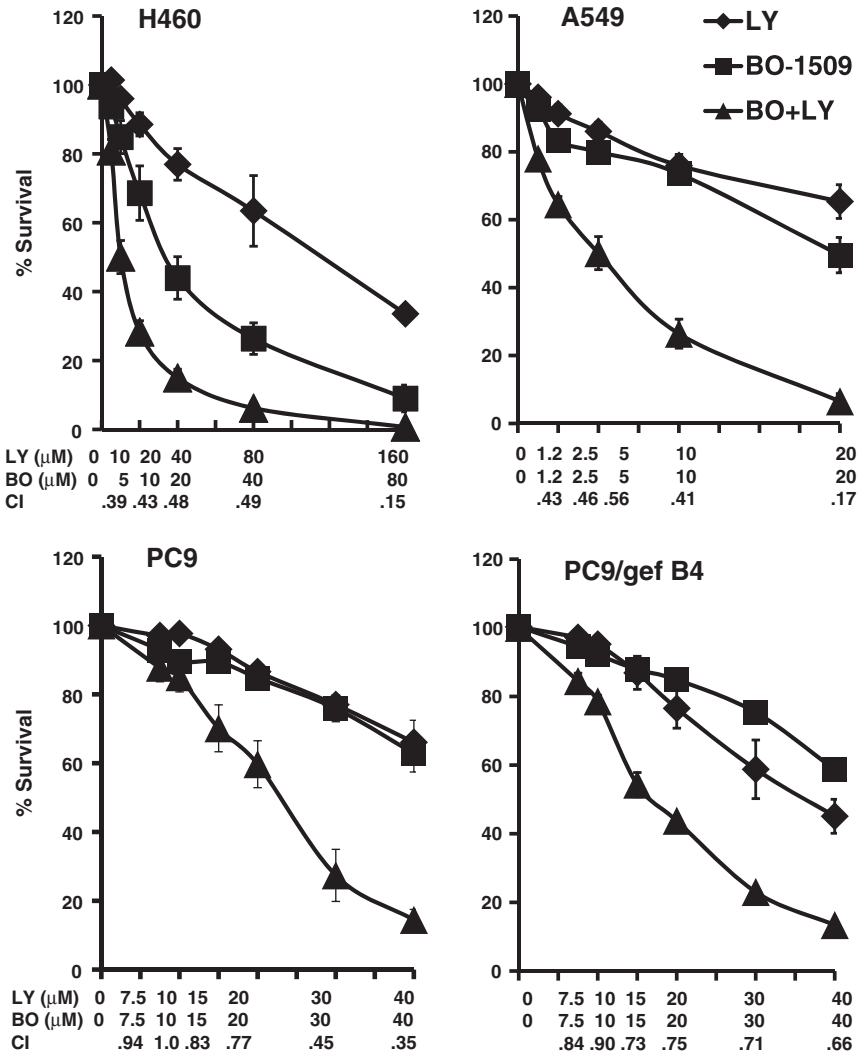

Figure 4. Synergistic killing with BO-1509 and LY294002. H460, A549, PC9, and PC9/gef B4 cells were treated for 72 hours with various concentrations of BO-1509 and LY294002 either alone or in combination. Cell viability was determined using the Alamar Blue assay. The numbers under the abscissa axis indicated the concentrations of BO-1509 and LY294002 used as either alone or in combination. The CIs of BO-1509 and LY294002 were determined using the Chou-Talalay software.

increase in FANCD2 protein levels was only observed in BO-1509–treated H460 and PC9/gef B4 cells. These results revealed that the modulation of levels of several repair proteins in response to DNA damage varied in different lung cancer cell lines treated with BO-1509.

Suppression of BO-1509–Induced DNA Repair Proteins by LY294002

PI3K signaling is one of the upstream regulatory pathways of the DDR [45]. Because BO-1509 treatment caused DNA damage and activated various repair molecules in different cells, we conducted experiments to determine whether the BO-1509–activated DNA repair components could be suppressed by the PI3K inhibitor LY294002 [46]. As shown in Figure 2, BO-1509 treatment resulted in an increase in pNbs1 and Rad51 that was suppressed by LY294002 at 40 μM in H460, A549, PC9, and PC9/gef B4 cells. In H460 cells, the BO-1509–induced up-regulation of Mre11 and FANCD2 was also suppressed by LY294002. Consistent with the results shown in Figure 1, there was no significant change in the protein levels of Rad50. By treatment of H460 cells with BO-1509, we also observed significantly increased Rad51 foci in nuclei by immunofluorescence staining (Figure 3*A*), implying that Rad51 was translocated into nuclei in response to BO-1509–induced DNA injury. However, LY294002 significantly reduced the Rad51 foci in the nucleus in BO-1509–treated H460 cells (Figure 3*A*). Similar findings were demonstrated in CL1-5 cells (Figure W2). Furthermore, we isolated nuclei and performed Western blot analysis to confirm the inhibitory effects of LY294002 on Rad51 translocation into nuclei. As shown in Figure 3*B*, Rad51 was remarkably increased in nuclear fraction of cells treated with BO-1509 alone, whereas BO-1509–enhanced Rad51 in nuclei was significantly suppressed by LY294002. These results indicate that inhibition of PI3K signaling by LY294002 counteracted the BO-1509–induced activation of DNA DSB repair machinery in various cell types.

Synergism between BO-1509 and the PI3 Kinase Inhibitor LY294002

While we observed a suppression of the DDR by the PI3K inhibitor LY294002, we next conducted experiments to monitor the cytotoxic effects of the combination treatment of BO-1509 and

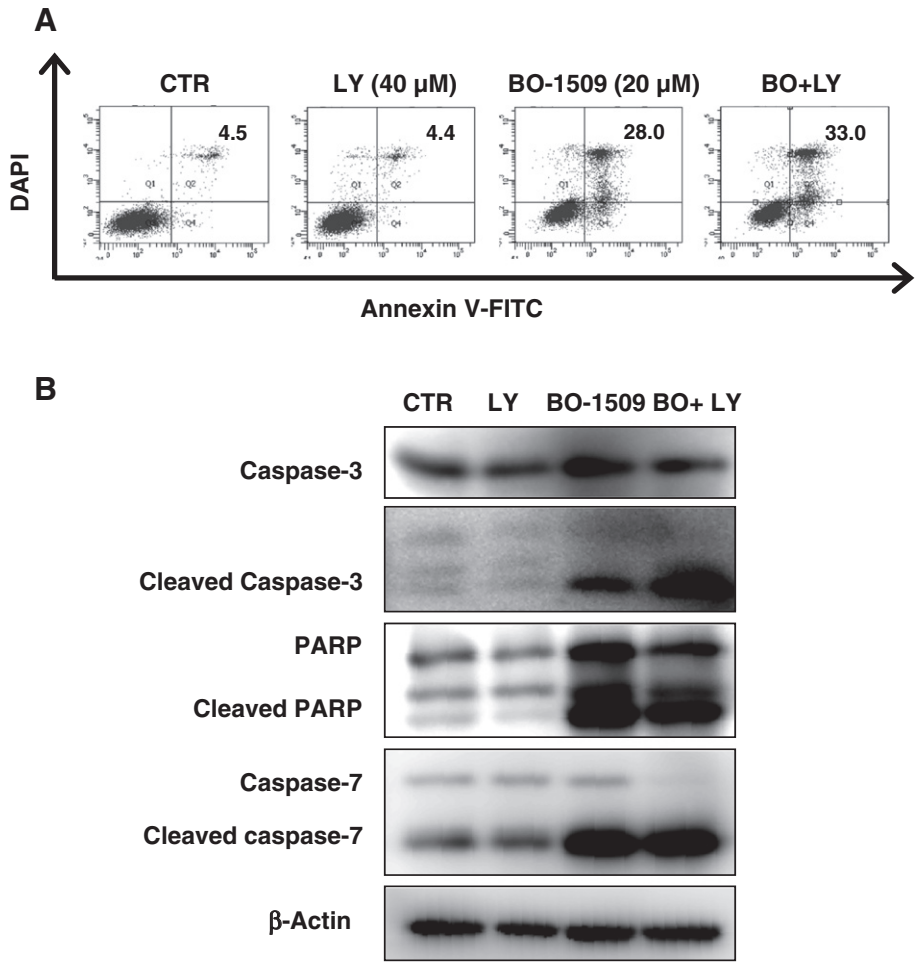

Figure 5. Increased apoptotic cell death in H460 cells treated with the combination of BO-1509 and LY294002. (A) Flow cytometry analysis of apoptotic cell death. H460 cells were treated with BO-1509 and LY294002 for 24 hours as described in Figure 2. At the end of the treatment, the cells were harvested and subjected to apoptosis analysis using the Annexin V–FITC Apoptosis Detection Kit. The numbers in the right corner indicate the percentage of apoptotic cells (i.e., Annexin V–positive cells). (B) Activation of apoptosis-executing proteins. As described in A, the cleaved forms of caspase-3, caspase-7, and PARP were detected by Western blot analysis. β-Actin was included as a loading control.

LY294002 in H460, A549, PC9, and PC9/gef B4 cells. These studies generated IC_{50} values of LY294002 for each of the following cell lines: H460 (111.2 ± 15.1 μM), A549 (28.4 ± 4.3 μM), PC9 (56.9 ± 1.1 μM), and PC9/gef B4 (31.3 ± 3.8 μM). As shown in Figure 4, the CIs were below 1 for all of the cell lines that were examined, indicating that the synergistic killing activity of the combination treatment of BO-1509 with LY294002 was cell line independent. Furthermore, we observed a significant increase in the number of apoptotic cells (Annexin V–positive population in the bottom and top right quadrants of the plot) in H460 cells co-treated with BO-1509 and LY294002 for 72 hours in comparison to cells treated with the individual drugs alone (Figure 5*A*). However, among apoptotic executive proteins, such as caspase-3, caspase-7, and PARP, we only observed significant increase of cleaved caspase-3 in H460 cells co-treated with BO-1509 and LY294002 compared to those treated with BO-1509 alone. Similar results using PC9 cells were shown in Figure W3. Therefore, we may infer that combination treatment with BO-1509 and LY294002 also triggers other death mechanisms. These results therefore indicate that inhibition of PI3K signaling enhanced the cytotoxic effect of BO-1509 in lung cancer cell lines.

Accumulation of DNA Damage by LY294002 in BO-1509–Treated Cells

The level of γH2AX is a well-documented hallmark of DNA double-strand breakage [47]. Using γH2AX as a biomarker, we used immunofluorescence staining and Western blot analysis to determine the effect of LY294002 on the repair of BO-1509–induced DNA damage. Because BO-1509 is a direct DNA-damaging agent, we therefore treated H460, PC9, and PC9/gef B4 cells for 2 hours and then incubated them with or without LY294002. In this study, γH2AX foci were used as an indicator of DNA damage. γH2AX-positive cells, which were designated as having more than five γH2AX foci per nucleus, were remarkably increased in H460, PC9, and PC9/gef B4 cells after treatment with BO-1509 for 2 hours followed by incubation in drug-free medium for 24 hours (Figure 6, *A*–*C*). However, the frequency of γH2AX-positive cells declined when these cells were incubated with drug-free medium for longer periods of up to 72 hours. γH2AX-positive cells at 72 hours were not apparently reduced in cells treated with both BO-1509 and LY294002 but significantly higher than those without LY294002 treatment (Figure 6, *A*–*C*). These results indicate that LY294002 suppresses the repair of BO-1509–induced DNA damage. Western blot assays

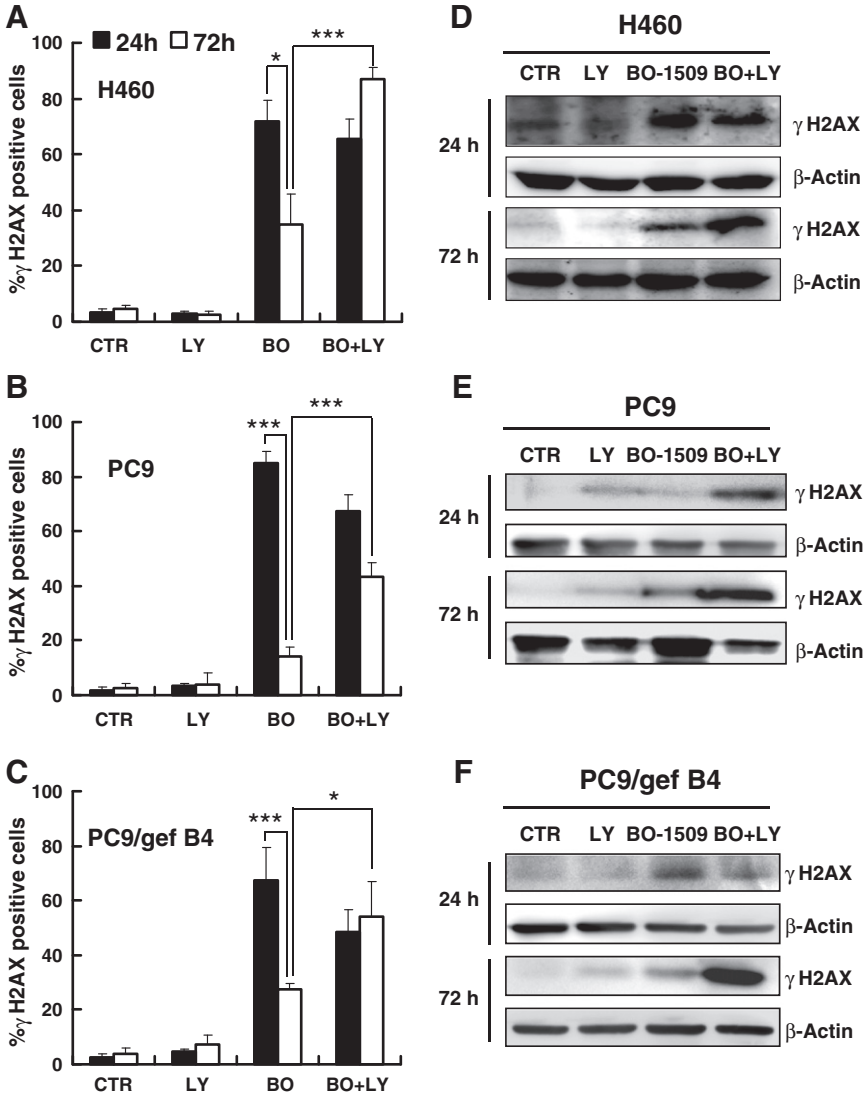

Figure 6. Inhibition of DNA repair by LY294002. H460 (A, D), PC9 (B, E), and PC9/gef B4 (C, F) cells were treated with 20 μM BO-1509 for 2 hours, washed, and then treated with or without 40 μM LY294002 for 24 or 72 hours. (A–C) Nuclear γH2AX foci determination. At the end of the treatment, the cells were fixed and stained with a primary antibody against γH2AX and then with an Alexa Fluor 488–conjugated secondary antibody (green). Nuclei were counterstained with DAPI (blue). The γH2AX-positive cells (more than five γH2AX foci per nucleus) were observed using a fluorescent microscope. *$P < .05$ and ***$P < .001$. (D–F) Western blot analysis of the H2AX protein. At the end of the treatment, the cells were lysed and subjected to Western blot analysis using an antibody against γH2AX as described in the Materials and Methods section. β-Actin was included as a loading control.

consistently showed elevated protein levels of γH2AX in H460, PC9, and PC9/gef B4 cells treated with the combination of BO-1509 and LY294002 for 72 hours in comparison to cells treated with BO-1509 alone (Figure 6, *D–F*). These results support the idea that LY294002 interferes with DNA repair and increases DSB damage in BO-1509–treated lung cancer cells.

Increased Antitumor Activity of BO-1509 by LY294002 in Mice Xenografted with Lung Cancer Cells

Because we observed a synergistic cytotoxicity of BO-1509 with LY294002 in H460, A549, PC9, and PC9/gef B4 cells *in vitro*, we further investigated the therapeutic efficacy of the combination treatment of BO-1509 and LY294002 in mouse xenograft models. When the subcutaneously implanted tumor size reached approximately 100 mm^3 for H460 cells, 70 mm^3 for PC9 and PC9/gef B4 cells, and 200 mm^3 for A549 xenografts, mice were treated with BO-1509 (5 mg/kg i.v., every other day times five), LY294004 (40 mg/kg i.p., 10 times daily), or a combination of both compounds [BO-1509 (5 mg/kg i.v., every other day times five) + LY294004 (40 mg/kg i.p., 10 times daily)]. As shown in Figure 7*A*, BO-1509 alone significantly suppressed the tumor burden by approximately 50% to 70%, whereas the effects of LY294002 alone on the suppression of the tumor burden were limited, except in PC9/gef B4–xenografted mice where an approximate 40% suppression was observed. In contrast, when BO-1509 was combined with LY294002, tumor growth was further suppressed in all of the tumor mouse xenografts with the exception of the PC9-xenografted mice (Figure 7*A*). Although PC9 cells were the most BO-1509–resistant cells in the *in vitro* cytotoxicity assay system, they showed the greatest suppression by BO-1509 in the mouse xenograft model.

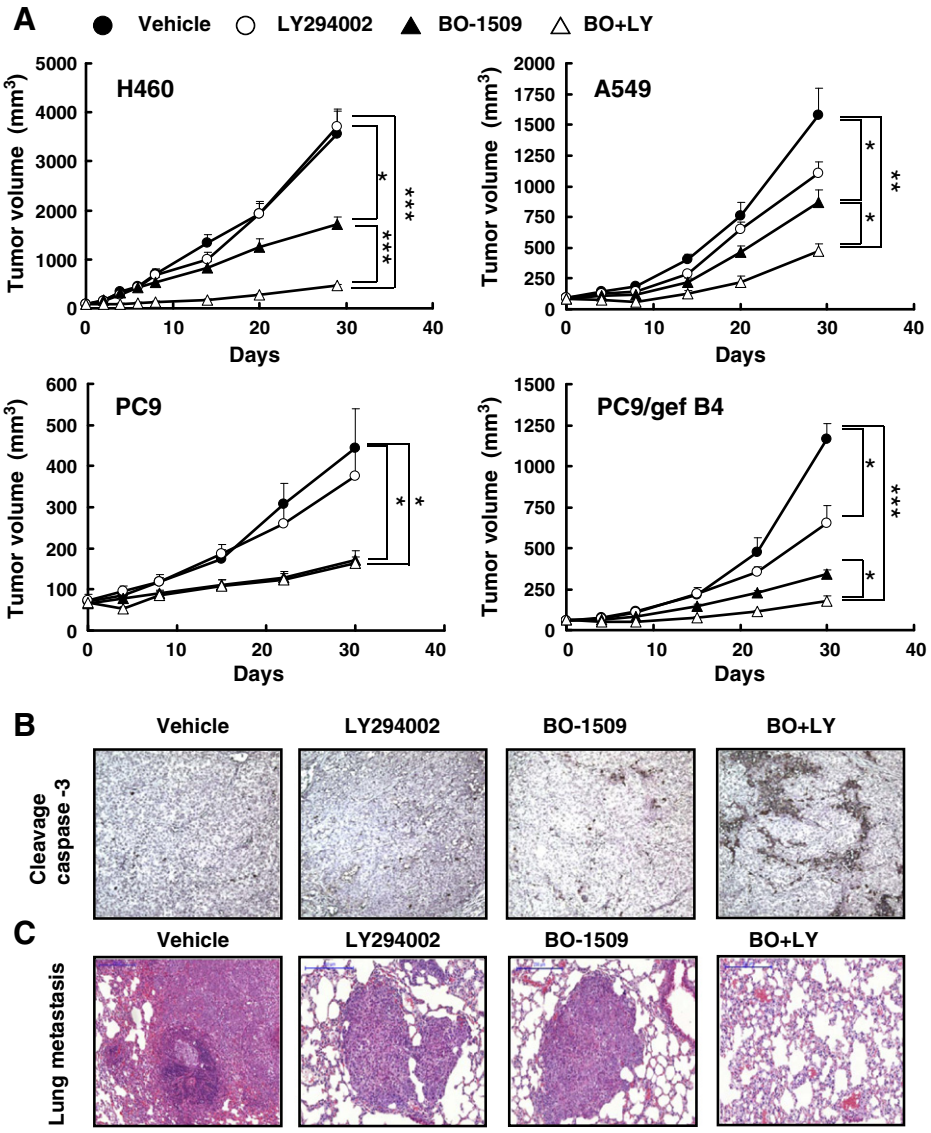

Figure 7. Therapeutic effects of BO-1509 and LY294002, either alone or in combination, in various lung cancer cells. (A) Suppression of tumor growth. Nude mice bearing H460, A549, PC9, or PC9/gef B4 cells were treated with vehicle, BO-1509 (5 mg/kg i.v., every other day times five), LY294002 (40 mg/kg i.p., 10 times daily), or the combination of BO-1509 and LY294002. The tumor size was determined as described in the Materials and Methods section. Student's *t*-test was used to determine the significance of the differences between the drug-treated group and vehicle group. $*P < .05$, $**P < .01$, and $***P < .001$. (B) Immunohistochemical staining of cleaved caspase-3. H460 tumors 24 hours after the last treatment protocol were harvested, sectioned, and stained with an antibody against cleaved caspase-3. (C) Lung tissue section. Twenty-nine days after transplantation, lung tissues from mice exposed or not to the drug treatments were harvested and examined by staining with hematoxylin and eosin (H&E).

On the 10th day of treatment (24 hours after the final treatment), the drug-treated H460-xenografted tumors were harvested and subjected to histopathologic examination. Using an antibody targeting the cleaved form of caspase-3, we observed a remarkable increase in active caspase-3 in tumor tissue harvested from mice treated with a combination of BO-1509 and LY294002 (Figure 7*B*). In contrast, little cleavage of caspase-3 was detected in tumor sections from mice treated with either BO-1509 or LY294002 alone. We also performed histopathologic examinations of various organs harvested from H460-xenografted mice on the 29th day. Significant metastasis was observed in the lungs of vehicle control (80%)–treated mice and mice treated with BO-1509 (67%) or LY294002 (80%) alone. In contrast, no metastatic foci were observed in the lungs of mice co-treated with BO-1509 and LY294002 (Figure 7*C*). We followed the combination-treated mice for 63 days and did not observe metastasis in the lungs.

Limited Adverse Effects of the Combination Treatment of BO-1509 and LY294002 in Xenografted Mice

Severe body weight reduction was not observed in any of the treatment groups (Figure W4). To determine whether our treatment regimen causes severe adverse effects, we performed histopathologic examinations of various organs harvested from H460-xenografted mice treated with BO-1509, LY294002, or both BO-1509 and LY294002 on the 10th day of treatment. No major pathologic or

Table 1. Blood Profiles on the 10th Day in BALB/c Nude Mice Treated with BO-1509, LY294002, or Both BO-1509 and LY294002.

Blood Parameters	Unit	Control	LY294002	BO-1509	BO-1509 + LY294002
WBCs	$10^3/\mu l$	3.06 ± 0.20	2.37 ± 0.20	1.80 ± 0.10	2.13 ± 0.60
Neutrophils	$10^3/\mu l$	1.16 ± 0.10	1.27 ± 0.10	1.06 ± 0.10	1.48 ± 0.40
Lymphocytes	$10^3/\mu l$	1.55 ± 0.20	0.81 ± 0.10	0.44 ± 0.10	0.32 ± 0.10
Monocytes	$10^3/\mu l$	0.18 ± 0.01	0.15 ± 0.05	0.22 ± 0.04	0.25 ± 0.06
Eosinophils	$10^3/\mu l$	0.05 ± 0.01	0.06 ± 0.01	0.02 ± 0.01	0.03 ± 0.00
Basophils	$10^3/\mu l$	0.12 ± 0.02	0.07 ± 0.00	0.03 ± 0.00	0.03 ± 0.00
RBCs	$10^6/\mu l$	10.32 ± 0.30	10.53 ±0.10	8.22 ± 0.30	7.96 ± 0.20
Hemoglobin	g/dl	15.85 ± 0.70	16.25 ± 0.10	12.73 ± 0.50	12.40 ± 0.10
Hematocrit	%	54.13 ± 1.60	54.1 ± 0.70	43.14 ± 1.10	41.50 ± 0.50
Mean cell volume	Fl	52.46 ± 0.30	51.5 ± 0.30	52.70 ± 0.50	52.20 ± 0.70
Mean cell hemoglobin	Pg	15.36 ± 0.40	15.40 ± 0.09	15.40 ± 0.16	15.63 ± 0.30
Mean corpuscular hemoglobin concentration	g/dl	29.30 ± 0.50	29.90 ± 0.30	29.30 ± 0.40	29.93 ± 0.44
RBC distribution width	%	20.32 ± 0.40	20.90 ± 1.00	18.46 ± 0.80	18.83 ± 0.70
Platelets	$10^3/\mu l$	847 ± 79	783 ± 86	1227 ± 298	1242 ± 151

Various blood parameters were measured in the blood of BALB/c nude mice on the second day after the end of treatment. Data indicate the means ± SD.

inflammatory changes were observed in the heart, kidney, lung, liver, or spleen by either macroscopic or microscopic examination (Figure W5). We also determined the complete blood profile and analyzed specific blood enzymes to determine whether any toxicity was present. As summarized in Table 1, mice treated with BO-1509, LY294002, or both BO-1509 and LY294002 showed leukocytopenia to varying degrees. Treatment of mice with LY294002 did not have any deleterious effects on the hematopoietic system because the red blood cell (RBC) count and hemoglobin concentration showed minimal changes. In contrast, the RBC count and hemoglobin concentration decreased by approximately 20% in mice treated with BO-1509 alone or with the combination of BO-1509 and LY294002.

Although thrombocytopenia is one of the most common toxic effects of DNA-alkylating agents, BO-1509 alone or in combination with LY294002 did not show thrombocytopenia; rather, a slight increase was observed in the number of platelets. However, mice treated with LY294002 showed slight thrombocytopenia. We also measured the levels of the biochemical enzymes alanine aminotransferase, aspartate aminotransferase (AST), lactate dehydrogenase (LDH), glucose, and blood urea nitrogen in mice treated with vehicle, BO-1509, LY294002, and the combination of BO-1509 and LY294002. As shown in Table 2, AST levels were slightly increased in mice treated with LY294002, whereas LDH levels were increased in the sera of the combination-treated mice. These results indicate limited toxicity for BO-1509 applied alone and in combination with LY294002 in mice.

Discussion

Derivatives of 3a-aza-cyclopenta[*a*]indenes are synthetic bifunctional alkylating agents that induce ICLs in DNA and are potent anticancer agents [30,31]. ICLs may cause replication-dependent DSB formation in DNA [4,48]. Cells undergo apoptosis if DNA DSBs are not repaired [4]. BO-1509 was synthesized through lead optimization of BO-1012, which was previously reported to have potent antitumor activity both *in vitro* and in tumor xenograft models. In the present study, we found that BO-1509 was more cytotoxic to H460 cells than BO-1012 (IC_{50} = 63.8 μM) [28].

Table 2. Blood Enzymes on the 10th Day in BALB/c Nude Mice Treated with BO-1509, LY294002, or the Combination of BO-1509 and LY294002.

Enzyme	Unit	Control	LY294002	BO-1509	BO-1509 + LY294002
AST	U/l	60.0 ± 10.0	75.6 ± 17.8	60.0 ± 6.3	67.3 ± 2.5
Alanine aminotransferase	U/l	33 ± 2.0	31.6 ± 2.5	28.6 ± 1.0	27.3 ± 6.3
LDH	U/l	381 ± 50	463 ± 117	473 ± 8	695 ± 155
Blood urea nitrogen	mg/dl	23.2 ± 0.2	25.0 ± 5.8	18.6 ± 1.3	17.7 ± 3.1
Glucose (GLU-P)	mg/dl	160 ± 1	172 ± 23	145 ± 19	132 ± 5

Various blood enzyme activities were measured in the blood of BALB/c nude mice on the second day after the end of treatment. Data indicate the means ± SD.

We also demonstrated that treatment of various human lung cancer cells with BO-1509 resulted in an increase in γH2AX protein (a well-established marker of DNA DSB) levels together with nuclear foci formation. Multiple repair pathways, including HR and NHEJ [4], are activated in response to the formation of DSB. In the four lung cancer cell lines examined, BO-1509 treatment activated Nbs1 and enhanced the expression and nuclear translocation of Rad51. However, the response of other repair components, such as Mre11 and FANCD2, to BO-1509–induced damage was different in different cell lines. The MRN complex functions as a DNA damage sensor [49], where FANCD2, a member of Fanconi anemia family that is an inherited genomic instability disorder, coordinates HR, nucleotide excision repair, and mutagenic translesion synthesis [50,51]. However, it is unclear why they have differential responses to DNA damage in different cell lines and it warrants our further investigation. LY294002, an inhibitor of PI3K signaling, significantly suppressed BO-1509–activated DNA repair protein levels and synergistically enhanced the cytotoxicity of BO-1509 in all of the cell lines that were studied. Inhibition of DNA repair pathway regulatory signaling is therefore a rational strategy for cancer treatment.

It has been reported that PI3K mediates the activation of ATM to facilitate DNA repair when DNA damage is induced by ionizing radiation [52]. LY294002 has been evaluated in various cell lines for its ability to inhibit all major subclasses of PI3K and PI3K-like kinases (ATM, ataxia telangiectasia and rad3 related, and DNA-dependent protein kinase) [27]. Furthermore, LY294002 has been used either alone or in combination with different chemotherapeutic drugs in *in vitro* and in preclinical studies [21,23,26,53]. These studies have shown that LY294002 can overcome the problem of drug resistance [53] and increase the efficacy of individual drugs in mouse tumor xenograft models [25,26]. Our present study has shown that LY294002 is able to enhance the killing effects of BO-1509. We also demonstrated that LY294002 mediates its effects through suppression of Nbs1 and Rad51, which are involved in the HR repair pathway [54-57]. In addition, Nbs1 is not only a core member of the

MRN complex that tethers DSB ends and recruits other proteins to conduct HR and NHEJ repair [7,58,59] but also plays specific roles in the activation of ATM and its downstream targets to trigger a second wave of repair [60].

In the present animal study, LY294002 alone did not induce any significant tumor reduction, with the exception of the PC9/gef B4 xenografts. In contrast, LY294002 enhanced the antitumor activity of BO-1509 in various lung cancer xenografts. The main goals of synergistic therapeutics are to decrease the dose of the individual drugs, reduce toxicity, minimize or delay the induction of drug resistance, and overcome the problem of drug resistance [61], and combination drug therapies have frequently been used for the treatment of a variety of cancers. Hematopoietic toxicity is major side effect of DNA-alkylating agents [62,63]. Similar to other alkylating agents, the treatment of mice with BO-1509 alone or in combination with LY294002 resulted in a moderate suppression of bone marrow–derived cells (i.e., a decrease in white blood cells (WBCs), RBCs, and hemoglobin). Although most alkylating agents cause a decrease in platelet count [62,63] as one of their side effects, BO-1509 did not suppress the platelet count. Furthermore, no major pathologic changes were observed in mice treated with the drugs alone or in combination. The combination of BO-1509 and LY294002 suppressed tumor metastasis, which is a crucial determinant of chemotherapy failure. Because LY294002 is not suitable for clinical use, the therapeutic efficacy of BO-1509 combined with other clinically approved PI3K inhibitors warrants further investigation.

Lung cancer is a major cause of cancer death and accounts for approximately 13% of all cancer deaths around the world because of its high incidence and mortality rates [64]. NSCLC contributes to approximately 85% of all lung cancers [38,65]. DNA-damaging drugs such as cisplatin, carboplatin, mitomycin C, and paclitaxel are typically the first lines of treatment for NSCLC, either alone or in combination [38,66]. However, less than 30% of patients respond to platinum-based chemotherapy. The main reason for the nonresponsiveness of chemotherapeutic agents in NSCLC is the intrinsic resistance to chemotherapy and radiation therapy [31]. Currently, TKIs such as gefitinib and erlotinib work well in patients who possess an EGFR deletion mutation in the Leu-Arg-Glu-Ala motif in exon 19 or a point mutation in exon 21 [67]. However, progression-free survival is only approximately 12 months, and acquired resistance frequently develops in the treated patients [68,69]. In the present study, the combination of BO-1509 and LY294002 significantly suppressed the growth of gefitinib-resistant PC9/gef B4 lung cancer cells and blocked tumor metastasis. These results suggest that this alternative therapeutic strategy may have the potential to serve as a third-line regimen against lung cancer.

In summary, our present study has shown that the combination of a DNA ICL agent with a PI3K inhibitor that inhibits DNA repair may be a feasible strategy to treat lung cancer, even for patients with acquired resistance to targeted therapy.

Acknowledgments

The authors thank the Pathological Core Laboratory, which is supported by the Institute of Biomedical Sciences, Academia Sinica. The authors also thank the Taiwan Mouse Clinic, which is funded by the National Research Program for Genomic Medicine at the National Science Council, R.O.C., for their excellent technical assistance on pathologic, hematological, and biochemical analyses.

References

[1] Chabner BA and Roberts Jr TG (2005). Timeline: chemotherapy and the war on cancer. *Nat Rev Cancer* **5**, 65–72.

[2] Califano R, Abidin AZ, Peck R, Faivre-Finn C, and Lorigan P (2012). Management of small cell lung cancer: recent developments for optimal care. *Drugs* **72**, 471–490.

[3] Hoy SM (2012). Bendamustine: a review of its use in the management of chronic lymphocytic leukaemia, rituximab-refractory indolent non-Hodgkin's lymphoma and multiple myeloma. *Drugs* **72**, 1929–1950.

[4] Helleday T, Petermann E, Lundin C, Hodgson B, and Sharma RA (2008). DNA repair pathways as targets for cancer therapy. *Nat Rev Cancer* **8**, 193–204.

[5] Brulikova L, Hlavac J, and Hradil P (2012). DNA interstrand cross-linking agents and their chemotherapeutic potential. *Curr Med Chem* **19**, 364–385.

[6] Lord CJ and Ashworth A (2012). The DNA damage response and cancer therapy. *Nature* **481**, 287–294.

[7] Stracker TH and Petrini JH (2011). The MRE11 complex: starting from the ends. *Nat Rev Mol Cell Biol* **12**, 90–103.

[8] Chan DA and Giaccia AJ (2011). Harnessing synthetic lethal interactions in anticancer drug discovery. *Nat Rev Drug Discov* **10**, 351–364.

[9] Engelman JA, Luo J, and Cantley LC (2006). The evolution of phosphatidylinositol 3-kinases as regulators of growth and metabolism. *Nat Rev Genet* **7**, 606–619.

[10] Deng R, Tang J, Ma JG, Chen SP, Xia LP, Zhou WJ, Li DD, Feng GK, Zeng YX, and Zhu XF (2011). PKB/Akt promotes DSB repair in cancer cells through upregulating Mre11 expression following ionizing radiation. *Oncogene* **30**, 944–955.

[11] Kao GD, Jiang Z, Fernandes AM, Gupta AK, and Maity A (2007). Inhibition of phosphatidylinositol-3-OH kinase/Akt signaling impairs DNA repair in glioblastoma cells following ionizing radiation. *J Biol Chem* **282**, 21206–21212.

[12] Tsai MS, Kuo YH, Chiu YF, Su YC, and Lin YW (2010). Down-regulation of Rad51 expression overcomes drug resistance to gemcitabine in human non-small-cell lung cancer cells. *J Pharmacol Exp Ther* **335**, 830–840.

[13] Toulany M, Kehlbach R, Florczak U, Sak A, Wang S, Chen J, Lobrich M, and Rodemann HP (2008). Targeting of AKT1 enhances radiation toxicity of human tumor cells by inhibiting DNA-PKcs-dependent DNA double-strand break repair. *Mol Cancer Ther* **7**, 1772–1781.

[14] Bakkenist CJ and Kastan MB (2003). DNA damage activates ATM through intermolecular autophosphorylation and dimer dissociation. *Nature* **421**, 499–506.

[15] Horejsi Z, Falck J, Bakkenist CJ, Kastan MB, Lukas J, and Bartek J (2004). Distinct functional domains of Nbs1 modulate the timing and magnitude of ATM activation after low doses of ionizing radiation. *Oncogene* **23**, 3122–3127.

[16] Liu P, Cheng H, Roberts TM, and Zhao JJ (2009). Targeting the phosphoinositide 3-kinase pathway in cancer. *Nat Rev Drug Discov* **8**, 627–644.

[17] Yap TA, Garrett MD, Walton MI, Raynaud F, de Bono JS, and Workman P (2008). Targeting the PI3K-AKT-mTOR pathway: progress, pitfalls, and promises. *Curr Opin Pharmacol* **8**, 393–412.

[18] Prevo R, Deutsch E, Sampson O, Diplexcito J, Cengel K, Harper J, O'Neill P, McKenna WG, Patel S, and Bernhard EJ (2008). Class I PI3 kinase inhibition by the pyridinylfuranopyrimidine inhibitor PI-103 enhances tumor radiosensitivity. *Cancer Res* **68**, 5915–5923.

[19] Garcia-Echeverria C and Sellers WR (2008). Drug discovery approaches targeting the PI3K/Akt pathway in cancer. *Oncogene* **27**, 5511–5526.

[20] Goodarzi AA and Lees-Miller SP (2004). Biochemical characterization of the ataxia-telangiectasia mutated (ATM) protein from human cells. *DNA Repair (Amst)* **3**, 753–767.

[21] Hu L, Zaloudek C, Mills GB, Gray J, and Jaffe RB (2000). In vivo and in vitro ovarian carcinoma growth inhibition by a phosphatidylinositol 3-kinase inhibitor (LY294002). *Clin Cancer Res* **6**, 880–886.

[22] Jiang H, Fan D, Zhou G, Li X, and Deng H (2010). Phosphatidylinositol 3-kinase inhibitor(LY294002) induces apoptosis of human nasopharyngeal carcinoma in vitro and in vivo. *J Exp Clin Cancer Res* **29**, 34.

[23] Bondar VM, Sweeney-Gotsch B, Andreeff M, Mills GB, and McConkey DJ (2002). Inhibition of the phosphatidylinositol 3′-kinase-AKT pathway induces apoptosis in pancreatic carcinoma cells in vitro and in vivo. *Mol Cancer Ther* **1**, 989–997.

[24] Semba S, Itoh N, Ito M, Harada M, and Yamakawa M (2002). The in vitro and in vivo effects of 2-(4-morpholinyl)-8-phenyl-chromone (LY294002), a specific

inhibitor of phosphatidylinositol 3′-kinase, in human colon cancer cells. *Clin Cancer Res* **8**, 1957–1963.
[25] Zhang H, Chen D, Ringler J, Chen W, Cui QC, Ethier SP, Dou QP, and Wu G (2010). Disulfiram treatment facilitates phosphoinositide 3-kinase inhibition in human breast cancer cells in vitro and in vivo. *Cancer Res* **70**, 3996–4004.
[26] Hu L, Hofmann J, Lu Y, Mills GB, and Jaffe RB (2002). Inhibition of phosphatidylinositol 3′-kinase increases efficacy of paclitaxel in in vitro and in vivo ovarian cancer models. *Cancer Res* **62**, 1087–1092.
[27] Lee CM, Fuhrman CB, Planelles V, Peltier MR, Gaffney DK, Soisson AP, Dodson MK, Tolley HD, Green CL, and Zempolich KA (2006). Phosphatidylinositol 3-kinase inhibition by LY294002 radiosensitizes human cervical cancer cell lines. *Clin Cancer Res* **12**, 250–256.
[28] Kakadiya R, Dong H, Lee PC, Kapuriya N, Zhang X, Chou TC, Lee TC, Kapuriya K, Shah A, and Su TL (2009). Potent antitumor bifunctional DNA alkylating agents, synthesis and biological activities of 3a-aza-cyclopenta[*a*] indenes. *Bioorg Med Chem* **17**, 5614–5626.
[29] Lai KC, Chang KW, Liu CJ, Kao SY, and Lee TC (2008). IFN-induced protein with tetratricopeptide repeats 2 inhibits migration activity and increases survival of oral squamous cell carcinoma. *Mol Cancer Res* **6**, 1431–1439.
[30] Sanjiv K, Su TL, Suman S, Kakadiya R, Lai TC, Wang HY, Hsiao M, and Lee TC (2012). The novel DNA alkylating agent BO-1090 suppresses the growth of human oral cavity cancer in xenografted and orthotopic mouse models. *Int J Cancer* **130**, 1440–1450.
[31] Lee PC, Kakadiya R, Su TL, and Lee TC (2010). Combination of bifunctional alkylating agent and arsenic trioxide synergistically suppresses the growth of drug-resistant tumor cells. *Neoplasia* **12**, 376–387.
[32] Muniandy PA, Liu J, Majumdar A, Liu ST, and Seidman MM (2010). DNA interstrand crosslink repair in mammalian cells: step by step. *Crit Rev Biochem Mol Biol* **45**, 23–49.
[33] Falasca M (2010). PI3K/Akt signalling pathway specific inhibitors: a novel strategy to sensitize cancer cells to anti-cancer drugs. *Curr Pharm Des* **16**, 1410–1416.
[34] Kurtz JE and Ray-Coquard I (2012). PI3 kinase inhibitors in the clinic: an update. *Anticancer Res* **32**, 2463–2470.
[35] Brambilla C and Spiro S (2001). Highlights in lung cancer. *Eur Respir J* **18**, 617–618.
[36] Saintigny P and Burger JA (2012). Recent advances in non-small cell lung cancer biology and clinical management. *Discov Med* **13**, 287–297.
[37] Stahel R, Peters S, Baas P, Brambilla E, Cappuzzo F, De Ruysscher D, Eberhardt WE, Felip E, Fennell D, and Marchetti A, et al (2013). Strategies for improving outcomes in NSCLC: a look to the future. *Lung Cancer* **82**, 375–382.
[38] Cataldo VD, Gibbons DL, Perez-Soler R, and Quintas-Cardama A (2011). Treatment of non–small-cell lung cancer with erlotinib or gefitinib. *N Engl J Med* **364**, 947–955.
[39] Maemondo M, Inoue A, Kobayashi K, Sugawara S, Oizumi S, Isobe H, Gemma A, Harada M, Yoshizawa H, and Kinoshita I, et al (2010). Gefitinib or chemotherapy for non–small-cell lung cancer with mutated EGFR. *N Engl J Med* **362**, 2380–2388.
[40] Burris III HA (2009). Shortcomings of current therapies for non-small-cell lung cancer: unmet medical needs. *Oncogene* **28**(Suppl 1), S4–S13.
[41] Chang TH, Tsai MF, Su KY, Wu SG, Huang CP, Yu SL, Yu YL, Lan CC, Yang CH, and Lin SB, et al (2011). Slug confers resistance to the epidermal growth factor receptor tyrosine kinase inhibitor. *Am J Respir Crit Care Med* **183**, 1071–1079.
[42] Yeh CT, Wu AT, Chang PM, Chen KY, Yang CN, Yang SC, Ho CC, Chen CC, Kuo YL, and Lee PY, et al (2012). Trifluoperazine, an antipsychotic agent, inhibits cancer stem cell growth and overcomes drug resistance of lung cancer. *Am J Respir Crit Care Med* **186**, 1180–1188.
[43] Chou TC (2006). Theoretical basis, experimental design, and computerized simulation of synergism and antagonism in drug combination studies. *Pharmacol Rev* **58**, 621–681.
[44] Avondoglio D, Scott T, Kil WJ, Sproull M, Tofilon PJ, and Camphausen K (2009). High throughput evaluation of gamma-H2AX. *Radiat Oncol* **4**, 31.
[45] Cimprich KA and Cortez D (2008). ATR: an essential regulator of genome integrity. *Nat Rev Mol Cell Biol* **9**, 616–627.
[46] Vlahos CJ, Matter WF, Hui KY, and Brown RF (1994). A specific inhibitor of phosphatidylinositol 3-kinase, 2-(4-morpholinyl)-8-phenyl-4H-1-benzopyran-4-one (LY294002). *J Biol Chem* **269**, 5241–5248.
[47] Bonner WM, Redon CE, Dickey JS, Nakamura AJ, Sedelnikova OA, Solier S, and Pommier Y (2008). γH2AX and cancer. *Nat Rev Cancer* **8**, 957–967.
[48] Helleday T, Lo J, van Gent DC, and Engelward BP (2007). DNA double-strand break repair: from mechanistic understanding to cancer treatment. *DNA Repair (Amst)* **6**, 923–935.
[49] Bartkova J, Tommiska J, Oplustilova L, Aaltonen K, Tamminen A, Heikkinen T, Mistrik M, Aittomaki K, Blomqvist C, and Heikkila P, et al (2008). Aberrations of the MRE11-RAD50-NBS1 DNA damage sensor complex in human breast cancer: *MRE11* as a candidate familial cancer-predisposing gene. *Mol Oncol* **2**, 296–316.
[50] Jacquemont C and Taniguchi T (2007). The Fanconi anemia pathway and ubiquitin. *BMC Biochem* **8**(Suppl 1), S10.
[51] Moldovan GL and D'Andrea AD (2012). To the rescue: the Fanconi anemia genome stability pathway salvages replication forks. *Cancer Cell* **22**, 5–6.
[52] Irarrazabal CE, Burg MB, Ward SG, and Ferraris JD (2006). Phosphatidylinositol 3-kinase mediates activation of ATM by high NaCl and by ionizing radiation: role in osmoprotective transcriptional regulation. *Proc Natl Acad Sci U S A* **103**, 8882–8887.
[53] Shin JY, Kim JO, Lee SK, Chae HS, and Kang JH (2010). LY294002 may overcome 5-FU resistance via down-regulation of activated p-AKT in Epstein-Barr virus-positive gastric cancer cells. *BMC Cancer* **10**, 425.
[54] Nakada D, Matsumoto K, and Sugimoto K (2003). ATM-related Tel1 associates with double-strand breaks through an Xrs2-dependent mechanism. *Genes Dev* **17**, 1957–1962.
[55] Lee JH and Paull TT (2004). Direct activation of the ATM protein kinase by the Mre11/Rad50/Nbs1 complex. *Science* **304**, 93–96.
[56] Daboussi F, Dumay A, Delacote F, and Lopez BS (2002). DNA double-strand break repair signalling: the case of RAD51 post-translational regulation. *Cell Signal* **14**, 969–975.
[57] Haaf T, Golub EI, Reddy G, Radding CM, and Ward DC (1995). Nuclear foci of mammalian Rad51 recombination protein in somatic cells after DNA damage and its localization in synaptonemal complexes. *Proc Natl Acad Sci U S A* **92**, 2298–2302.
[58] Borde V and Cobb J (2009). Double functions for the Mre11 complex during DNA double-strand break repair and replication. *Int J Biochem Cell Biol* **41**, 1249–1253.
[59] Bressan DA, Baxter BK, and Petrini JH (1999). The Mre11-Rad50-Xrs2 protein complex facilitates homologous recombination-based double-strand break repair in *Saccharomyces cerevisiae*. *Mol Cell Biol* **19**, 7681–7687.
[60] Cartagena-Lirola H, Guerini I, Viscardi V, Lucchini G, and Longhese MP (2006). Budding yeast Sae2 is an in vivo target of the Mec1 and Tel1 checkpoint kinases during meiosis. *Cell Cycle* **5**, 1549–1559.
[61] Chou TC (2010). Drug combination studies and their synergy quantification using the Chou-Talalay method. *Cancer Res* **70**, 440–446.
[62] van der Wall E, Beijnen JH, and Rodenhuis S (1995). High-dose chemotherapy regimens for solid tumors. *Cancer Treat Rev* **21**, 105–132.
[63] Verweij J and Pinedo HM (1990). Mitomycin C: mechanism of action, usefulness and limitations. *Anticancer Drugs* **1**, 5–13.
[64] Jemal A, Bray F, Center MM, Ferlay J, Ward E, and Forman D (2011). Global cancer statistics. *CA Cancer J Clin* **61**, 69–90.
[65] Travis WD, Travis LB, and Devesa SS (1995). Lung cancer. *Cancer* **75**, 191–202.
[66] Clegg A, Scott DA, Hewitson P, Sidhu M, and Waugh N (2002). Clinical and cost effectiveness of paclitaxel, docetaxel, gemcitabine, and vinorelbine in non-small cell lung cancer: a systematic review. *Thorax* **57**, 20–28.
[67] Shepherd FA, Rodrigues Pereira J, Ciuleanu T, Tan EH, Hirsh V, Thongprasert S, Campos D, Maoleekoonpiroj S, Smylie M, and Martins R, et al (2005). Erlotinib in previously treated non–small-cell lung cancer. *N Engl J Med* **353**, 123–132.
[68] Nguyen KS, Kobayashi S, and Costa DB (2009). Acquired resistance to epidermal growth factor receptor tyrosine kinase inhibitors in non–small-cell lung cancers dependent on the epidermal growth factor receptor pathway. *Clin Lung Cancer* **10**, 281–289.
[69] Pao W and Chmielecki J (2010). Rational, biologically based treatment of *EGFR*-mutant non-small-cell lung cancer. *Nat Rev Cancer* **10**, 760–774.

Supplementary materials
Appendix A

Table W1. The Characteristics of NSCLC Lines Used in This Study

Cell Line	EGFR	TP53	Kras	EGFR-TKI Response
H460	WT	WT	Q61H	Intrinsic resistant
A549	WT	WT	G12S	Intrinsic resistant
CL1-5	WT	R248W	WT	Intrinsic resistant
PC9	Exon 19 deletion	WT	WT	Sensitive
PC9/gef B4	Exon 19 deletion	WT	WT	Resistant (slug overexpression)
CL83	WT	ND	WT	Intrinsic resistant
CL25	Exon 19 deletion	C135Y	WT	Sensitive

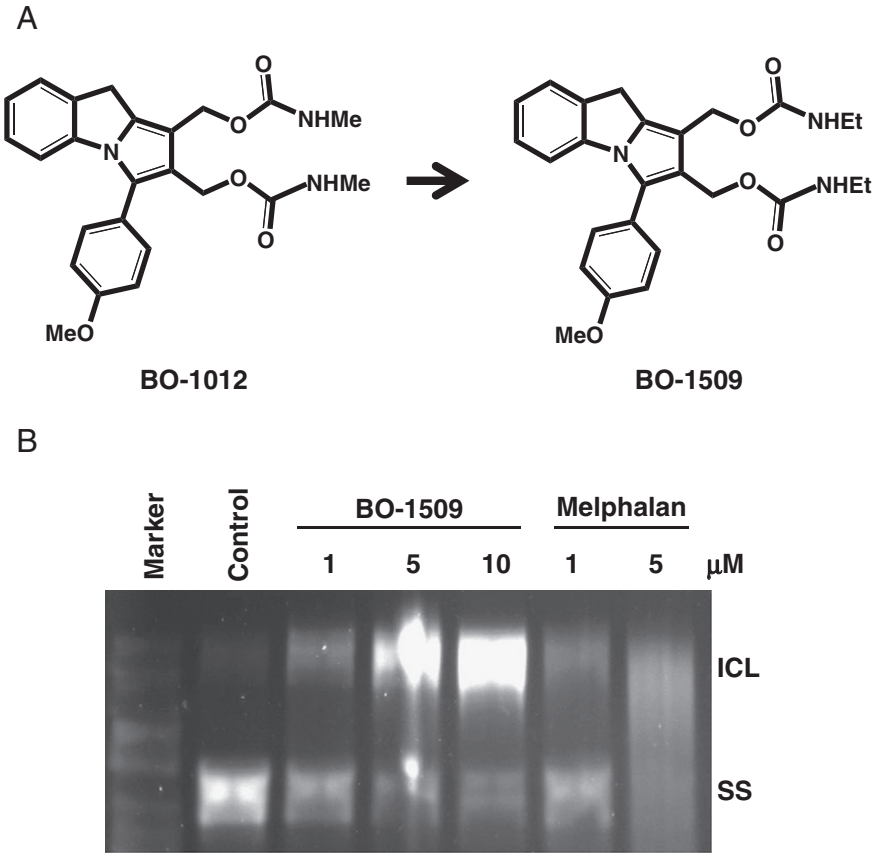

Figure W1. Chemical structure of BO-1509 and its activity on the induction of DNA interstrand cross-links. (A) The chemical structure of BO-1509 derived from BO-1012. (B) The DNA cross-linking activity of BO-1509 was analyzed by alkaline agarose gel electrophoresis. Melphalan was included for comparison. SS, single strand.

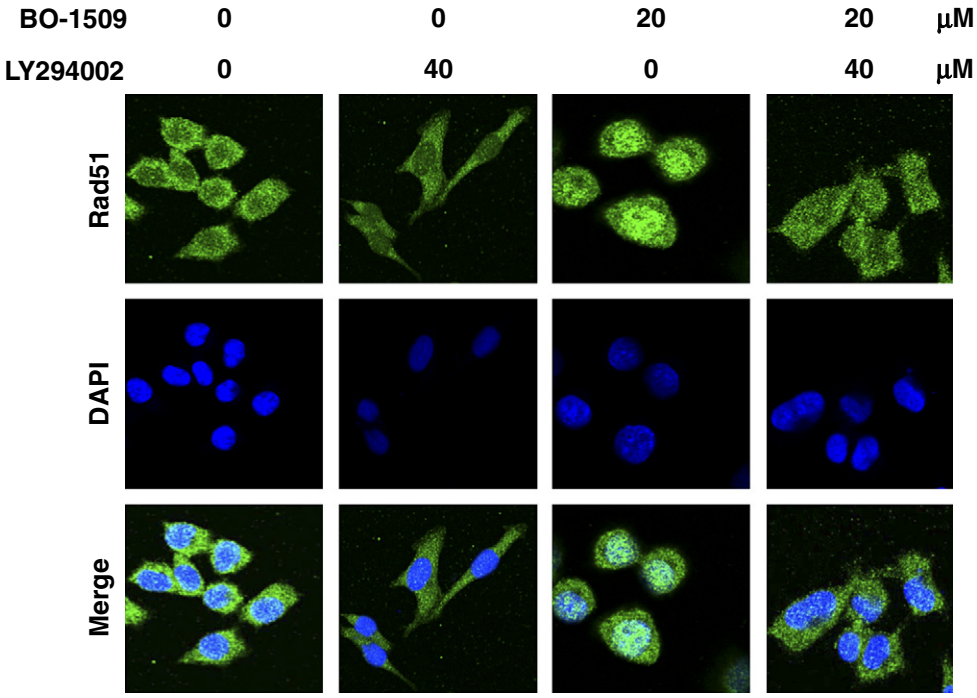

Figure W2. Inhibition of BO-1509–mediated Rad51 foci formation in the nuclei of CL1-5 cells. H460 cells grown on chamber slides were treated 20 μM BO-1509 for 2 hours, followed by treatment with or without 40 μM LY294002 for 24 hours. At the end of the incubation, the cells were fixed and stained with a primary antibody against Rad51 and an Alexa Fluor 488–conjugated secondary antibody (green). Nuclei were counterstained with DAPI (blue).

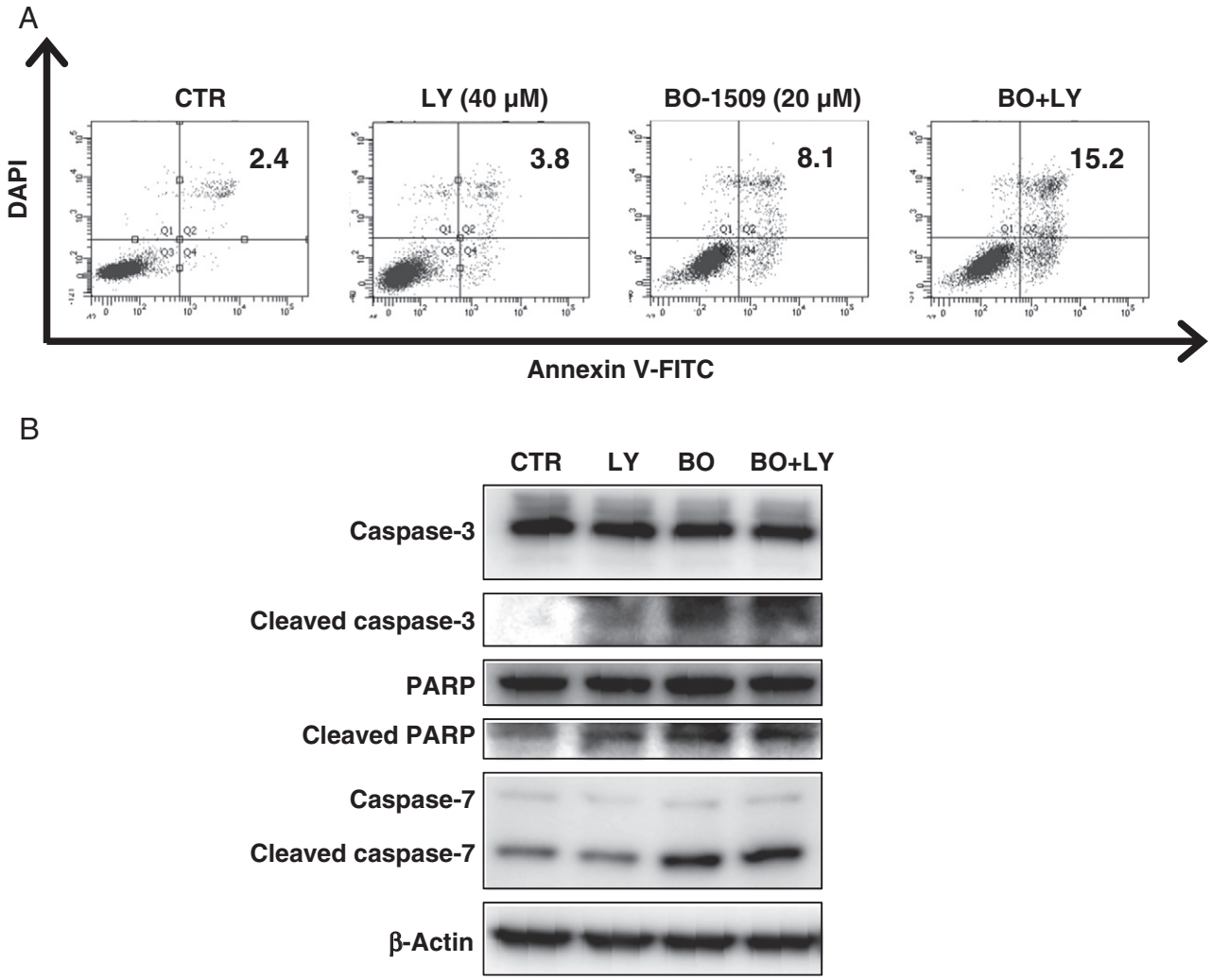

Figure W3. Increased apoptotic cell death PC9 cells treated with the combination of BO-1509 and LY294002. (A) Flow cytometry analysis of apoptotic cell death. PC9 cells were treated with BO-1509 (20 μM) and LY294002 (40 μM) together or alone for 48 hours. The numbers in the right corner indicate the percentage of apoptotic cells. (B) Activation of apoptosis-executing proteins. PC9 cells were treated with BO-1509 and LY294002 together or alone for 24 hours. The cleaved forms of caspase-3, caspase-7, and PARP were detected by Western blot analysis. β-Actin was included as a loading control.

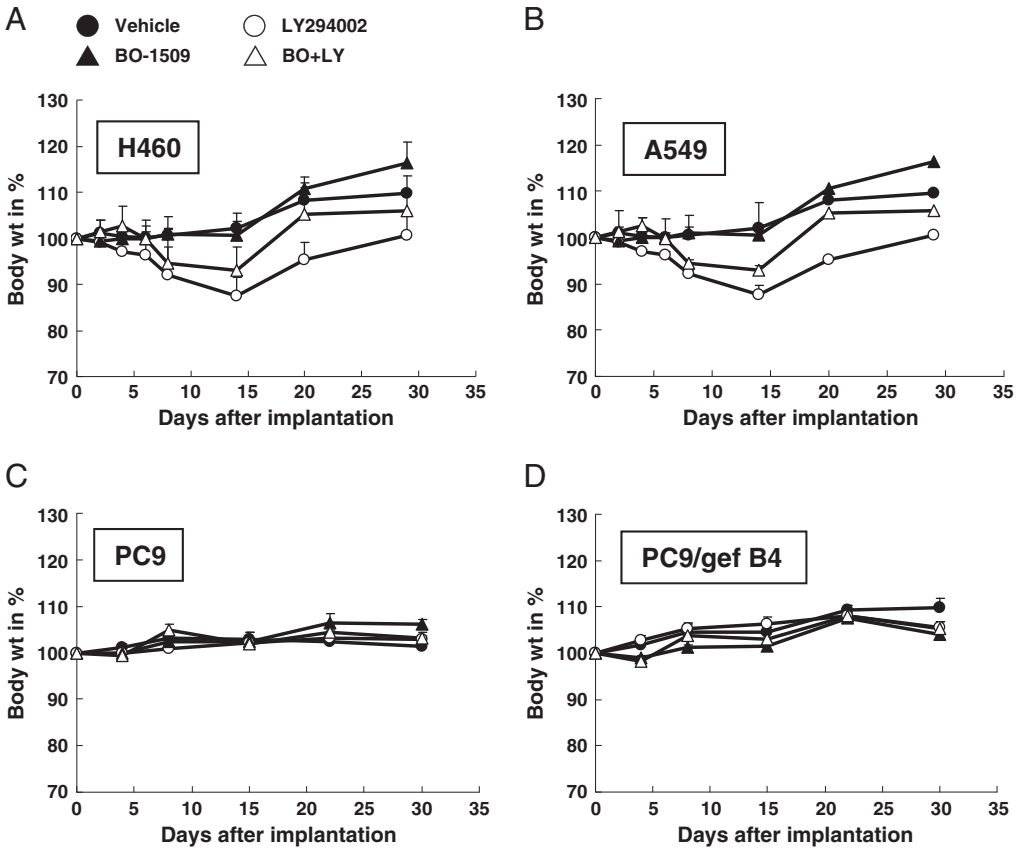

Figure W4. Body weight changes in tumor-bearing mice treated with BO-1509, LY294002, or the combination of BO-1509 and LY294002. (A) H460 cells. (B) A549 cells. (C) PC9 cells. (D) PC9/gef B4.

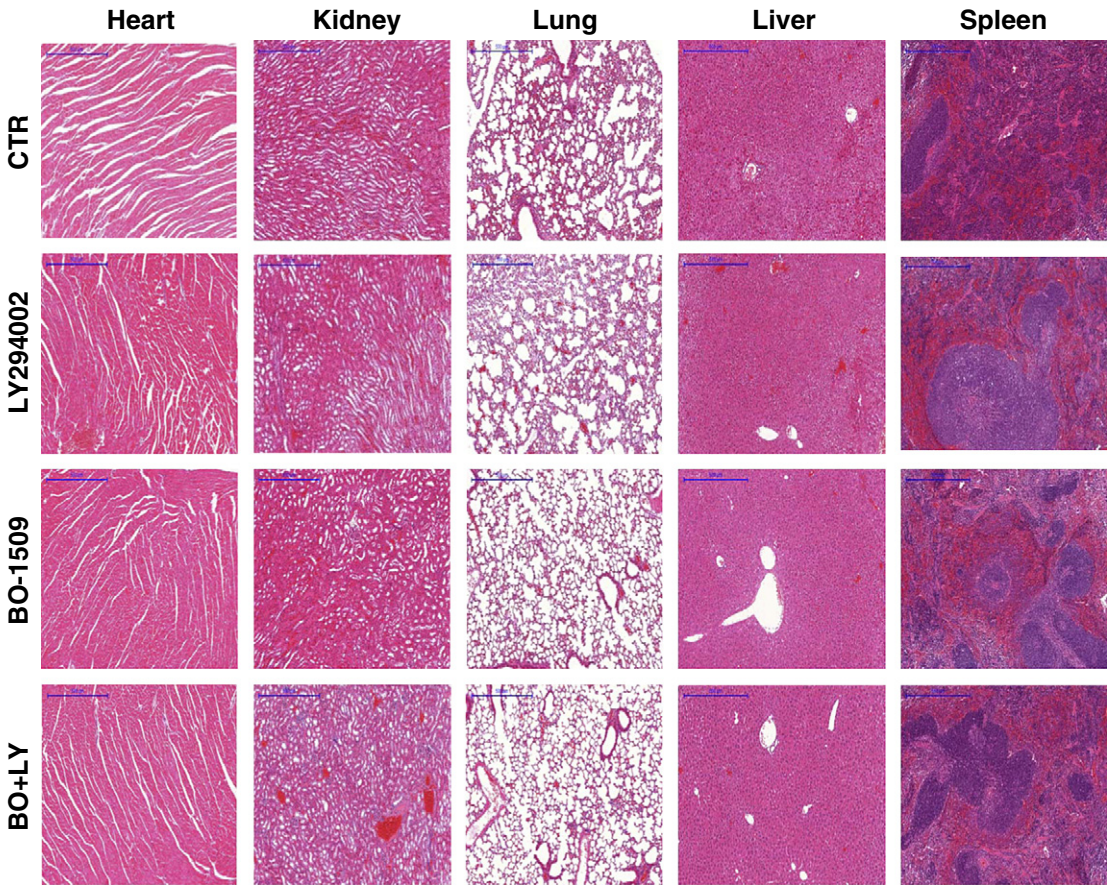

Figure W5. Acute and delayed toxicity of BO-1509, LY294002, and the combination of BO-1509 and LY294002 in various organs in nude mice. Different organs and tumors were harvested from nude mice treated with drugs on the 10th day of the experiment. Histopathologic sections from organs were stained with H&E and scanned. Scale bar, 500 μm.